




# Biodegradation of PLA/CNC composite modified with non-ionic surfactants

Gelsoeide da Silva Gois<sup>1</sup> · Amélia Severino Ferreira Santos<sup>2</sup>  · Eduardo Padrón Hernández<sup>3</sup> · Eliton Souto Medeiros<sup>2</sup> · Yeda Medeiros Bastos Almeida<sup>1</sup>

Received: 13 May 2022 / Revised: 14 November 2022 / Accepted: 22 November 2022 /  
Published online: 1 December 2022

© The Author(s), under exclusive licence to Springer-Verlag GmbH Germany, part of Springer Nature 2022

## Abstract

Poly(lactic acid) (PLA) undergoes degradation through the action of microorganisms and enzymes that can degrade it by composting. The goal of this work was to observe the degradation/disintegration behavior in garden soil of neat PLA and PLA composites with 3 wt% cellulose nanocrystals (CNC) modified or not with non-ionic surfactants (S) at a weight ratio of 1:1 (CNC:S). Four types of non-ionic surfactants with hydrophilic-lipophilic balance (HLB) ranging from 4.3 to 16.7 were tested: sorbitan monolaurate (Span 20), sorbitan monooleate (Span 80), polyoxyethylene sorbitan monolaurate (Tween 20) and polyoxyethylene sorbitan monooleate (Tween 80). Films were obtained by solution casting, cut into 2 × 2 cm strips and buried in garden soil, while monitoring the temperature and humidity for 150 days. Changes in the films by visual inspection, polarized light microscopy, thermogravimetric analysis (TGA) and Fourier-transform infrared spectroscopy (FTIR) were observed. Results showed that the addition of surfactants favored the rate of biodegradation of the composites, being the lowest molecular weight the determinant property of the surfactant to enhance biodegradation rate of PLA/CNC/S composites. Nevertheless, for surfactants belonging to the same chemical family, the highest biodegradation rate for PLA/CNC/S composite obeys the principle of high HLB, and low spherulite size.

**Keywords** Disintegration · Nanocrystal · Cellulose · HLB · Soil · Composting

✉ Amélia Severino Ferreira Santos  
amelia.santos@academico.ufpb.br

<sup>1</sup> Department of Chemical Engineering, Federal University of Pernambuco — UFPE, Av. Prof. Moraes Rego, 1235, Cidade Universitaria, Recife, PE 50670-901, Brazil

<sup>2</sup> Department of Materials Engineering, Federal University of Paraíba—UFPB, Cidade Universitaria, s/n Castelo Branco, João Pessoa, Paraíba, PB 58051-900, Brazil

<sup>3</sup> Department of Physics, Federal University of Pernambuco—UFPE, Av. Prof. Moraes Rego, 1235, Cidade Universitaria, Recife, PE 50670-901, Brazil

## Introduction

The excessive amount of municipal solid waste (MSW) produced and their appropriate disposal is one of the main current environmental. In this context, the increasing use of non-biodegradable and petroleum-based plastics for short product life cycle represents a significant part of this impact [1–3].

Biodegradable polymers in turn are susceptible to degradation caused by the action of microorganisms, leading to fragmentation, followed by mineralization (formation of carbon dioxide and/or methane, water, and biomass) [4]. Cellulose nanocrystals (CNC), together with biodegradable polymers from renewable resources attract attention of the scientific community for having a new perspective on a future scenario in the replacement of non-biodegradable plastics.

Poly(lactic acid) (PLA) is a biodegradable thermoplastic polyester produced from L-lactic acid—LLA (levorotatory) and D-lactic acid—DLA (dextrorotatory), being obtained both by chemical and biological methods and with applications in different areas [5]. According to the literature [6, 7], when a PLA product is properly disposed of, it undergoes hydrolysis, being converted into harmless natural products. The biodegradation time of PLA in the environment is from 6 months to 2 years, compared to 500 to 1000 years for conventional plastics, such as polystyrene and polyethylene [6].

The use of cellulose nanocrystals (CNC) occurs as a nano-reinforcement for the PLA matrix. The CNC consists of cellulose single crystals with high crystallinity, high surface area and nanometric dimensions. They are extracted from renewable sources, biodegradable, and widely used to improve the performance of polymers [8, 9]. Other authors [5, 9, 10] investigated the use of PLA/CNC nanocomposites and verified changes in the glass transition temperature and in Young's modulus of neat PLA. Fortunati et al. [10] studied PLA/CNC in the proportions of 99/1 and 97/3 and obtained an increase in Young's modulus by 21% and 55%, as well as an increase in glass transition temperature.

Several works [5, 11–14] present surfactants as an alternative to improve CNC dispersion in non-polar polymer matrices. The preparation consists of an aqueous suspension of CNC with surfactant, followed by freeze drying. The addition of surfactant can promote electrostatic repulsion or steric hindrance between particles, inhibiting their agglomeration into flakes during the freeze-drying process due to the strong hydrogen bonds.

In this study, the biodegradation of PLA composites with neat CNC (PLA/CNC) and CNC modified by nonionic surfactant (PLA/CNC/S) was evaluated. Four different types of surfactants were assessed using a constant amount of CNC and fixing the CNC-to-surfactant ratio. The biodegradation tests were carried out for 0, 90, 120 and 150 days in garden soil.

## Materials and methods

### Materials

Poly(lactic acid) (PLA) with melt flow index of  $80 \text{ g} \cdot 10 \text{ min}^{-1}$  ( $210 \text{ }^\circ\text{C}$ ,  $2.16 \text{ kg}$ ), was supplied by Cargil (Ingeo 3251D, Cargil S.A., USA). Commercial cotton linters were purchased from a local market and used as a source of cellulose for nanocrystals extraction. Analytical grade sulfuric acid ( $\text{H}_2\text{SO}_4$ , 95–97%, Química Moderna, Brazil) and chloroform (Vetec, Brazil) were used without further purification. Four types of non-ionic surfactants (Fig. 1) were used in this study: ALKEST SP20—sorbitan monolaurate (SP20, Oxiteno SA) with molecular weight of 346.5 Da and hydrophilic-lipophilic balance (HLB) of 8.6; ALKEST TW80—polyoxyethylene sorbitan monooleate (TW80, Oxiteno SA) with molecular weight of 1310 Da and HLB of 15; Tween 20—polyoxyethylene sorbitan monolaurate (TW20, BASF SA) with molecular weight of 1228 Da and HLB of 16.7; and Span 80—sorbitan monooleate (SP80, Sigma-Aldrich) with molecular weight of 428.6 Da and HLB of 4.3.

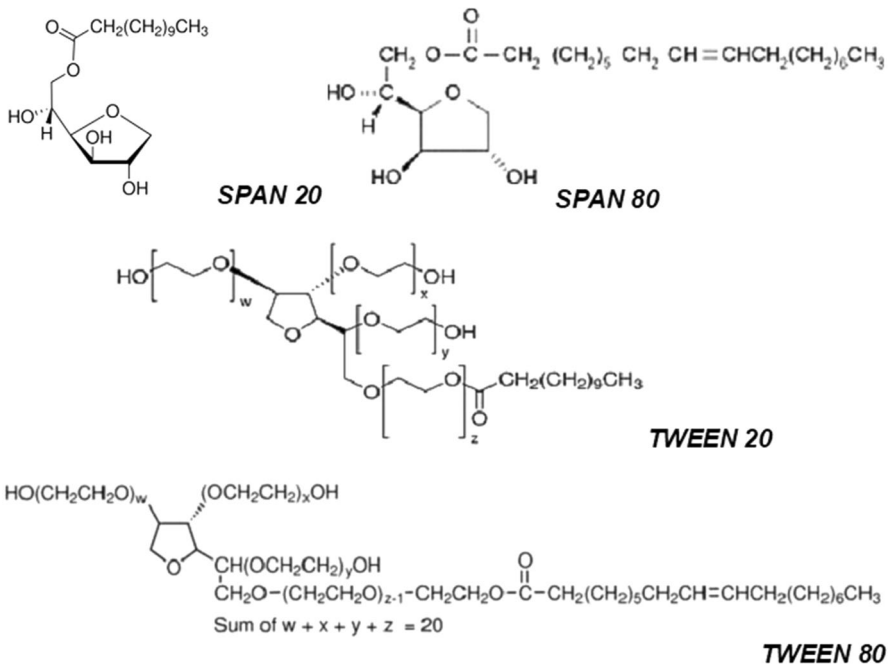


Fig. 1 Chemical structures of non-ionic surfactants used in this study. Source: Sigma-Aldrich

## Preparation of cellulose nanocrystals

Acid hydrolysis was carried out by adding 5 wt% cotton linters in 64 vol% sulfuric acid aqueous solution at 45 °C for 60 min under vigorous mechanical stirring [15]. Then, hydrolysis was stopped using an ice bath and adding deionized water in a dilution factor of 2:1. Excess acid was removed by repeated centrifugation cycles at 3000 rpm for 15 min (Centerium Scientific K3 Series). Afterwards, the resulting dispersion of CNC was dialyzed against running water until a neutral pH was reached. Part of the dialyzed aqueous dispersion was stored in a freezer, and the other part was diluted to 4 mg·mL<sup>-1</sup> in deionized water and freeze-dried in an LB 300TT equipment to obtain the neat CNC powder. Dry sample was stored in a desiccator at room temperature. According to Fig. 2, CNC had an average length and diameter of 209 ± 8 nm and 20 ± 1 nm, respectively, and aspect ratio 10 ± 0.5 nm, as determined previously by the authors [16]. Similar results were also found by Lizundia et al. [17].

## CNC modified with surfactants (CNC/S)

Surfactant modified CNC (CNC/S) were prepared by adding each surfactant to the dialyzed aqueous dispersion of CNC at a 1:1 weight ratio [12, 18, 19], based on a dry mass of nanocrystals. For adsorption to occur, dispersions were vigorously mixed using an Ultra Turrax (IKA T18 Basic) at 7000 rpm for 30 s. The obtained CNC/S dispersions were freeze-dried and stored similarly to neat CNC. The four

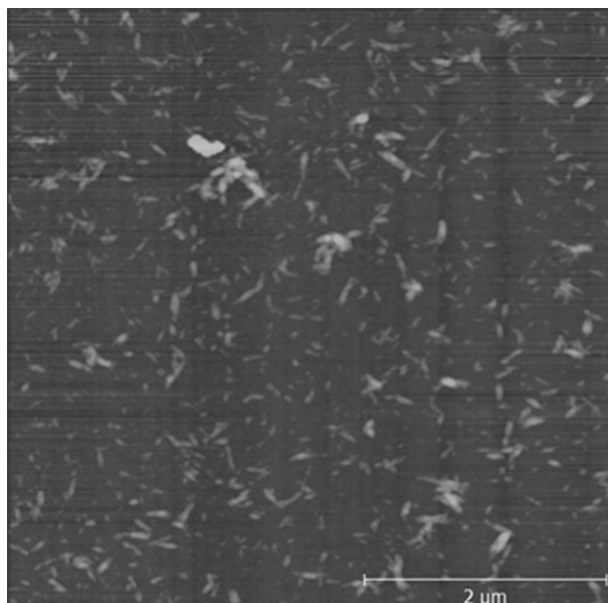


**Fig. 2** AFM images for neat CNC dispersed in water at 0.04 mg·mL<sup>-1</sup>

CNC samples containing surfactants were labeled as: CNC/SP20, CNC/SP80, CNC/TW20 and CNC/TW80.

### Preparation of PLA/CNC composites films

Films were prepared by solution casting method. Dispersions of neat CNC and CNC/S (1:1) in chloroform, prepared with cellulose nanocrystals content adjusted to obtain nanocomposites with 3 wt% CNC, were magnetically stirred and further, mixed with the previously prepared 10 wt% solution of PLA in chloroform and stirred for about 30 min. The neat PLA, PLA/CNC and PLA/CNC/S dispersions were poured onto glass Petri dishes greased with silicon ( $\varnothing$  15 cm) and left to evaporate for 48 h at room temperature. This concentration was chosen based on the literature reports [10, 18–20]. The PLA/CNC and PLA/CNC/S films presented a non-uniform dispersion with small agglomerates that are related to the weak interaction between hydrophilic CNC and hydrophobic PLA matrix [12, 18, 19, 21].

### Biodegradation test

Tests were carried out according to ASTM G 160-12. The garden soil used has a varied microbial flora with bacteria, fungi, yeasts, and presence of sporulated bacilli, confirmed by plate colony-counting method [22, 23]. In order to prove the microbial activity of the garden soil, tensile tests were performed on samples of cotton cloth to reach a tensile strength loss of at least 50% after burying them in the soil for 5 days.

Thus, after evaluating the adequacy of the soil, PLA, PLA/CNC and PLA/CNC/SP20, PLA/CNC/SP80, PLA/CNC/TW20 and PLA/CNC/TW80 films cut to approximately  $2 \times 2$  cm were buried for 90, 120, 150 and 180 days (180 days being analyzed only visually) [24]. During the test period, soil temperature and moisture were monitored weekly. The soil temperature remained around  $29 \pm 0.6$  °C and the soil moisture content was adjusted to  $28 \pm 6\%$ . The soil moisture content was determined by measuring their weight loss upon drying for 24 h at 105 °C. At the end of each exposure period, the specimens were removed from the soil bed and tested according to respective test method. For visual evaluation, the material is rinsed under a stream of tap water while gently rubbing between fingers to remove soil and dried at room conditions.

### Characterizations

The obtained films were characterized before and after each exposure period in biodegradation test by polarized light microscope (Leica ICC 50), using a magnification of up to 40 $\times$ . Thermogravimetric analysis (TGA) was performed using a Perkin Elmer simultaneous thermal analyzer STA6000. The samples were heated from room temperature to 700 °C at 10 °C $\cdot$ min $^{-1}$  in a nitrogen flow rate of 20 mL $\cdot$ min $^{-1}$ . The samples were analyzed in a Bruker Tensor 27 FTIR spectrophotometer, using 16 scans with resolution of 4 cm $^{-1}$  and interval of 2 cm $^{-1}$  using the attenuated total reflectance mode (ATR) by direct analysis of film on ZnSe

crystal. FTIR spectra were baseline-corrected, and ATR corrected. The carbonyl index was calculated by the ratio of the peak intensity at  $1748\text{ cm}^{-1}$  to the reference peak at  $1451\text{ cm}^{-1}$ .

## Results and discussion

### Soil microbial and standard microbial activity

Soil microbial population was evaluated to ensure the existence of soil microbiota, especially the presence of more resistant bacteria such as endospore producers. Figure 3A shows the photograph of the analysis of microorganisms in the garden soil. A mixed population with the presence of colonies of filamentous fungi, bacteria and yeasts can be observed in these photographs. The spore-producing bacteria were counted on a plate and 50,000 CFU (Colony Forming Unit) were quantified (Fig. 3B). The presence of spores was confirmed by spore staining (Fig. 3B) where bacteria (in the form of pink rods) and green spores can be visualized. These species survive in unfavorable environmental conditions, such as under nutrients or water scarcity. The resistance of these species assured the continuity of the biodegradation process.

Cotton specimens before and after 5 days of exposure to the garden soil presented a tensile strength of  $81 \pm 6\text{ MPa}$  and  $31 \pm 6\text{ MPa}$ , respectively. Therefore, a reduction in tensile strength by about 60% was achieved, which is in accordance with the ASTM G 160-12 requirement. Additionally, these characterizations proved that garden soil produces fungi and bacteria favorable to the polymer biodegradation, since they are capable of producing enzymes of the hydrolases class in polyesters that favor PLA hydrolysis.

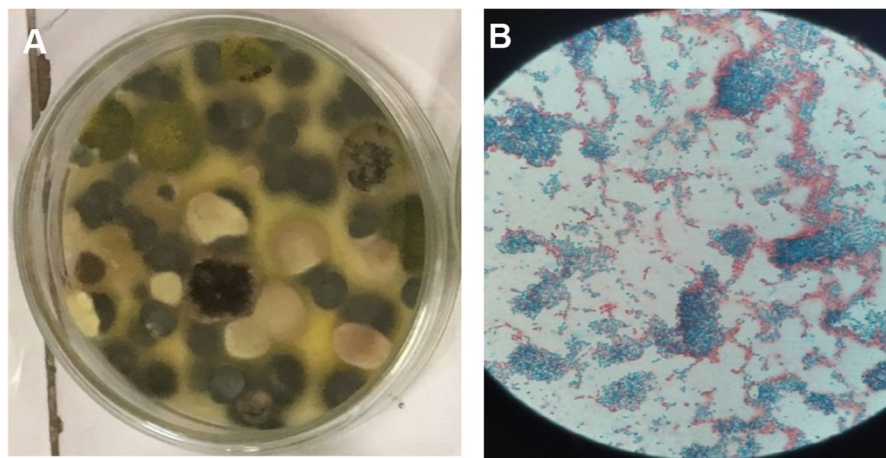


**Fig. 3** Image of microorganisms (A) and spore-producing bacteria (B) found in garden soil

### Visual inspection

Images of PLA and PLA/CNC, PLA/CNC/SP20, PLA/CNC/SP80, PLA/CNC/TW20 and PLA/CNC/TW8 films before and after 90, 120, 150 and 180 days of exposure to garden soil can be observed in Fig. 4. These images show film darkening as degradation goes on. This color change in the samples can possibly be attributed to absorption of water, presence of microorganisms and soil components that promote film fragility. According to Haque et al. [25], it is the presence of products formed in the hydrolytic process that induces a change in the refractive index and in film color.

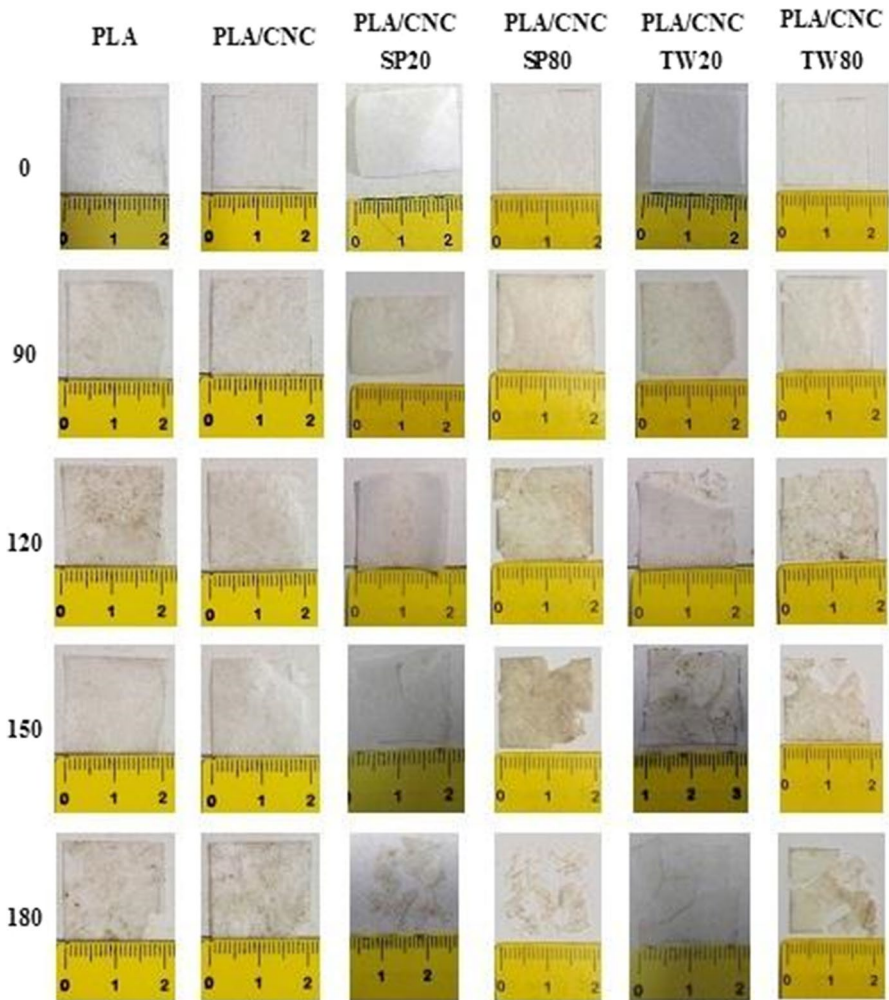


**Fig. 4** Photograph of PLA, PLA/CNC and PLA/CNC/S films before and after 90, 120, 150 and 180 days of exposure to garden soil

PLA has a slower degradation/disintegration rate compared to other biodegradable polyesters [26–28]. Rudnik and Briassoulis [27] explain that the microorganisms that degrade PLA are not easily found in natural environments, thus being less susceptible to microbial attack. Additionally, Farah et al. [28] explained that the steric effect of PLA's alkyl group hinders hydrolysis attack of its ester bonds.

As shown in the images, all samples showed biodegradation. Among the samples, the fragmentation rate of PLA/CNC/SP20, PLA/CNC/SP80, PLA/CNC/TW20 and PLA/CNC/TW80 composites was more noticeable than that observed for PLA/CNC and neat PLA. Therefore, it can be inferred that the surfactant accelerates the biodegradation of the polymer and could be a good choice to improve biodegradation rate of PLA, as already pointed out in our earlier study with PLA/CNC nanocomposites modified with ethylene oxide derivatives [29].

The surfactants possibly made the polymer more susceptible to microorganisms attack in the initial phase of disintegration, fostering hydrolysis. It is known that under composting conditions the disintegration process begins with the hydrolysis of the amorphous phase of the material [30, 31]. Nevertheless, two of the surfactants used in this study, SP20 and SP80, have an HLB value lower than 10 and thus, a hydrophobic/lipophilic character. The lowest HLB has a value of 4.3 (SP80). Conversely, they also have the lowest molecular weight and the longest alkyl chain end, which were less susceptible to hydrolysis, being equal to the respective TWEEN family, i.e., SP20 and TWEEN20, and SP80 and TWEEN80. The high molecular weight of the TWEEN family is attributed to 20 ethylene oxide units added to each hydroxyl unit of 1,4-sorbitan ( $C_6H_{12}O_5$ ), which make them hydrophilic, presenting HLB greater than 10.

Given these differences and similarities, Fig. 4 points out that PLA/CNC/SP20 and PLA/CNC/SP80 presented the fastest disintegration rate, since both samples were fully disintegrated into small pieces within 180 days. Therefore, considering the TWEEN and SPAN family of surfactants, the hydrophilic nature of surfactants was not the determinant property to enhance PLA/CNC biodegradation rate.

## Polarized light microscopy

Since the disintegration of PLA is already noticeable after 150 days of soil exposure (Fig. 4), the films before and after 150 days of biodegradation were chosen to be analyzed by polarized light microscopy (Fig. 5).

After 150 days of biodegradation, neat PLA maintained its morphology with degradation points throughout the film (yellow circles in Fig. 5). PLA/CNC and PLA/CNC/S showed more prominent changes in morphology exhibiting more degradation points (Fig. 5) throughout the film than that observed in neat PLA. These results confirm that garden soil was suitable for carrying out biodegradation tests.

According to Haque et al. [25], holes on the surface of the samples can be formed by the degradation of the interspherulitic or interlamellar amorphous phase due to enzymatic action. Since the size of PLA/CNC and PLA/CNC/S spherulites was lower than for neat PLA, the effect of CNC and CNC/S nucleation in the PLA composite possibly contributed to this behavior [21, 32, 33]. A close inspection of



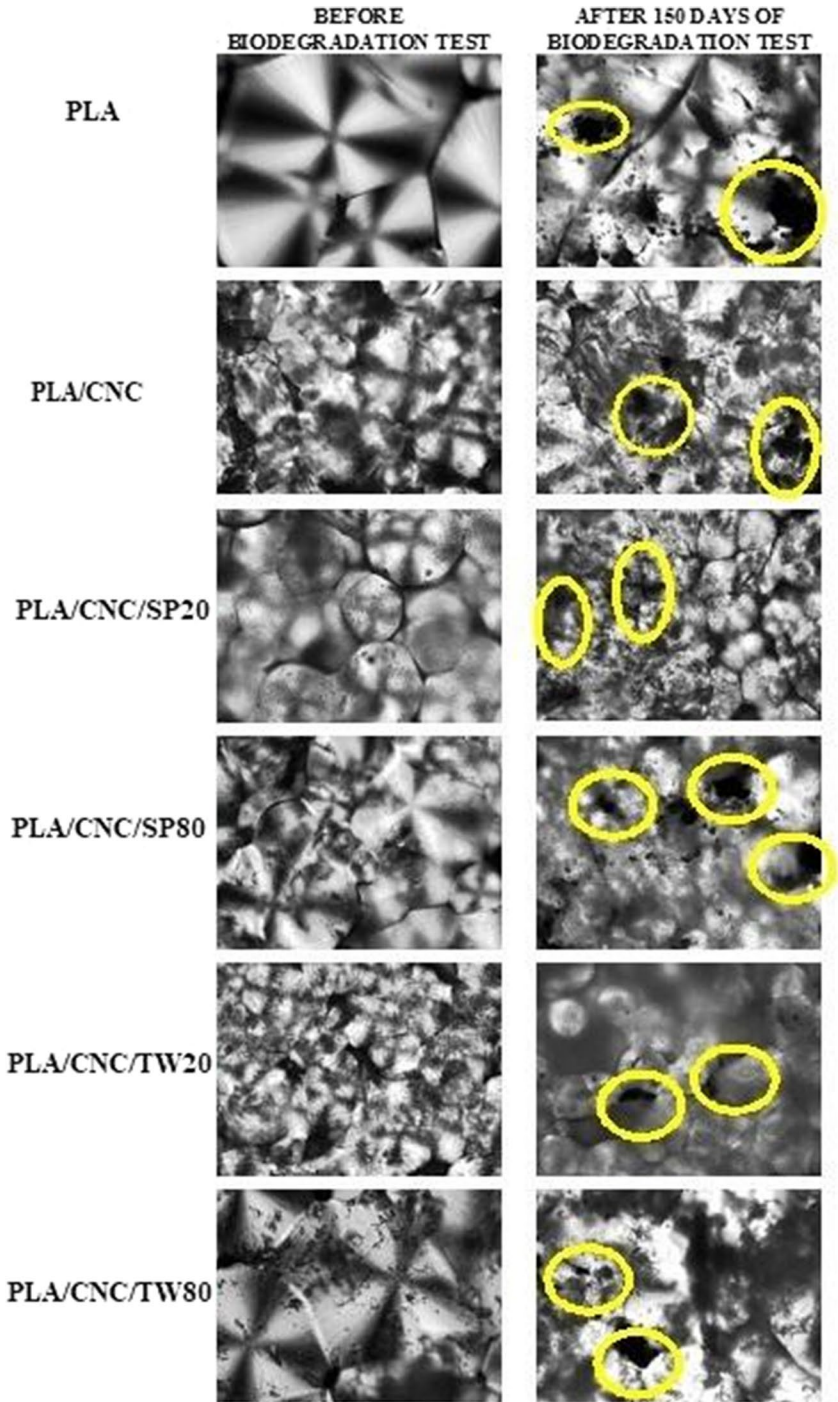


Fig. 5 Polarized light microscopy images of the films before and after 150 days of soil exposure

the morphology of PLA/CNC/S spherulites (Fig. 5) show that the PLA/CNC/SP20 and PLA/CNC/TW20 had a smaller spherulite size than PLA/CNC/SP80 and PLA/CNC/TW80. According to Gois [34], the crystallinity index of composites before biodegradation test in decrescent order is: PLA/CNC/TW80 (57%) > PLA/CNC/SP80 (53%) > PLA/CNC/SP20 (42%) > PLA/CNC/TW20 (36%). The neat PLA and PLA/CNC sample showed crystallinity degree of 48% and 54%, respectively. Therefore, PLA/CNC/SP20 and PLA/CNC/TW20 have crystallinity degree and a spherulite size smaller than neat PLA and PLA/CNC, which can increase susceptibility to biodegradation [35]. Nevertheless, PLA/CNC/SP20 showed the highest nucleation effect among surfactants [34], which is confirmed by its spherulitic morphology (Fig. 5).

Furthermore, the surfactant itself also increases the disintegration rate of the PLA/CNC/S composites during composting conditions and induces the formation of a porous structure in the PLA/CNC/S composites, since it is a low molecular weight compound that has relatively higher hydrophilicity compared to PLA [35]. Furthermore, according to Gu et al. [36], polymer additives could act as a source of carbon and energy for microorganisms, helping biodegradation to take place. Changes in porosity, crystallinity degree, crystalline morphology, and in surface polarity of composites, caused by the use of CNC/S, contribute to increase PLA accessibility to water and microorganisms, accelerating the hydrolysis process and enhancing the disintegration rate [21, 35].

### Thermogravimetric analysis (TGA)

The samples under composting conditions showed a decrease in the onset degradation temperature ( $T_{\text{onset}}$ ) and the maximum rate of decomposition temperature ( $T_{\text{max}}$ ) for all exposure times of the biodegradation test (Table 1), a similar result was found by Arrieta et al. [28].

**Table 1** Values of the onset degradation temperature ( $T_{\text{onset}}$ ) and temperature of the maximum rate of decomposition ( $T_{\text{max}}$ ) for neat PLA, PLA/CNC and PLA/CNC/S composites at different exposure time intervals in the soil

| Days                | Temperature (°C)   |                  |                    |                  |                    |                  |                    |                  |                    |                  |                    |                  |
|---------------------|--------------------|------------------|--------------------|------------------|--------------------|------------------|--------------------|------------------|--------------------|------------------|--------------------|------------------|
|                     | PLA                |                  | PLA/CNC            |                  | PLA/CNC<br>SP20    |                  | PLA/CNC<br>SP80    |                  | PLA/CNC<br>TW20    |                  | PLA/CNC<br>TW80    |                  |
|                     | $T_{\text{onset}}$ | $T_{\text{max}}$ | $T_{\text{onset}}$ | $T_{\text{max}}$ | $T_{\text{onset}}$ | $T_{\text{max}}$ | $T_{\text{onset}}$ | $T_{\text{max}}$ | $T_{\text{onset}}$ | $T_{\text{max}}$ | $T_{\text{onset}}$ | $T_{\text{max}}$ |
| 0                   | 327                | 359              | 323                | 354              | 336                | 359              | 313                | 345              | 311                | 367              | 312                | 343              |
| 90                  | 317                | 357              | 320                | 348              | 292                | 344              | 304                | 348              | 296                | 355              | 294                | 349              |
| 120                 | 312                | 358              | 314                | 346              | 293                | 341              | 298                | 345              | 296                | 357              | 289                | 343              |
| 150                 | 311                | 358              | 310                | 347              | 256                | 327              | 297                | 343              | 268                | 313              | 285                | 338              |
| TD (%) <sup>1</sup> | 4.9                | <1               | 4.0                | 2.0              | 23.8               | 8.9              | 5.1                | <1               | 13.8               | 14.7             | 8.6                | 1.4              |

<sup>1</sup>Temperature decrease (TD)—percentual difference between each temperature before and after 150 days of exposure in the soil relative to the respective temperature of the original sample

Comparing the onset degradation temperature of PLA and PLA/CNC, the addition of CNC did not significantly change the  $T_{onset}$  of PLA, collaborating with visual analysis (Fig. 3). Nevertheless, the addition of surfactants altered the  $T_{onset}$  of PLA, as observed by Arrieta et al. [28].

The most accentuated difference in  $T_{onset}$  was evidenced by PLA/CNC/SP20 with a decrease of 18% relative to neat PLA after 150 days of exposure in the soil, or 24% relative to its own initial  $T_{onset}$ , corroborating with the previous results of the visual inspection and optical microscopy (Figs. 3 and 4). The difference in  $T_{onset}$  of the other PLA/CNC/S composites relative to its own initial  $T_{onset}$  was less than 15%, being difficult to point out significant differences among them, and to correlate with previous results. It is noteworthy to point that PLA/CNC/TW20 presented the second highest reduction in the  $T_{onset}$  after 150 days of exposure in the soil relative to its own initial  $T_{onset}$ , but it could be more associated to its lowest crystallinity degree relative to all PLA/CNC/S composites.

Table 2 presents the values of molecular weight and HLB of each kind of surfactant, together with degree of crystallinity of each PLA/CNC/S and spherulite size based on an increasing scale from 1 (one) to 4 (four).

According to these data, SP20 presented the third highest HLB (8.6) and the lowest molecular weight (346.5 Da) among the surfactants, and PLA/CNC/SP20 is the composite with the second lowest crystallinity degree and the lowest spherulite size. Therefore, among the surfactant types evaluated, the molecular weight behaved as the determinant parameter to enhance biodegradation rate of PLA/CNC composite. However, for surfactants belonging to the same chemical family, Gois et al. [29] found the highest biodegradation rate for PLA/CNC/S composite with the highest HLB, i.e., hydrophilicity, regardless of surfactant molecular weight. Results found in this work also obeys the same principle when the same family (TWEEN or SPAN) was evaluated. Furthermore, all other properties are according to the literature [21, 32, 33, 36] criteria established to increase the biodegradation rate, i.e., low crystallinity, low spherulite size, and low molecular weight.

**Table 2** Values of molecular weight and HLB of each kind of surfactant, together with the crystallinity degree (Xc) of each PLA/CNC/S [34] and relative spherulite size

| Surfactant |                      | PLA/CNC/S |        |                              |
|------------|----------------------|-----------|--------|------------------------------|
| Type       | Mn (Da) <sup>a</sup> | HLB       | Xc (%) | Spherulite size <sup>b</sup> |
| SP20       | 346.5                | 8.6       | 42     | 1                            |
| SP80       | 428.6                | 4.3       | 53     | 3                            |
| TW20       | 1228                 | 16.7      | 36     | 2                            |
| TW80       | 1310                 | 15        | 57     | 4                            |

<sup>a</sup>Number average molecular weight

<sup>b</sup>Increasing scale from 1 to 4, where 1 and 4 is the smallest and largest spherulite size, respectively

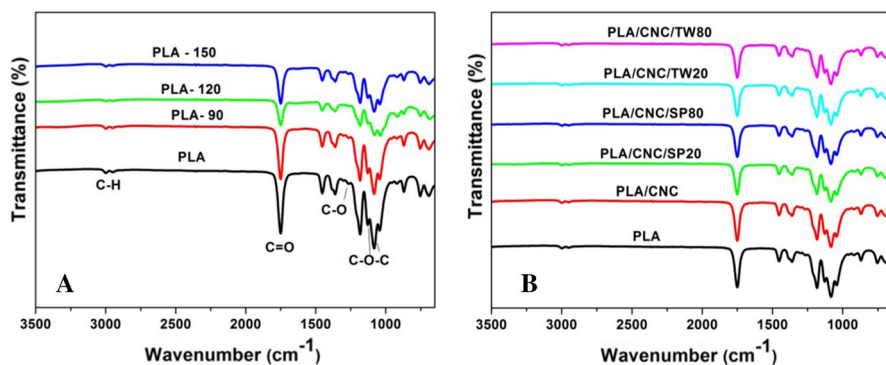


**Fig. 6** FTIR spectra of neat PLA before and after 90, 120 and 150 days of soil exposure (A) and FTIR of all films before soil exposure (B)

**Table 3** Values of carbonyl index of neat PLA and PLA composites films before and after different exposure time intervals in soil

| Days    | PLA  | PLA/CNC | PLA/CNC SP20 | PLA/CNC SP80 | PLA/CNC TW20 | PLA/CNC TW80 |
|---------|------|---------|--------------|--------------|--------------|--------------|
| 0       | 3.62 | 3.48    | 3.24         | 3.28         | 3.22         | 3.32         |
| 90      | 3.08 | 2.60    | 3.20         | 2.51         | 3.15         | 2.76         |
| 120     | 2.51 | 3.14    | 3.34         | 2.70         | 2.78         | 3.43         |
| 150     | 2.82 | 3.25    | 3.17         | 2.82         | 2.66         | 2.93         |
| CID (%) | 22.1 | 6.6     | 2.2          | 14.0         | 17.4         | 11.7         |

<sup>1</sup>Carbonyl Index decrease (CID)—percentual difference between carbonyl index of respective sample before and after 150 days of exposure in the soil relative to the respective carbonyl index of the original sample

### Fourier transform infrared spectroscopy (FTIR)

Fourier transform infrared spectroscopy in attenuated total reflection (ATR) mode was used to evaluate the chemical changes that occur on film surface. The spectra of all films before and after the soil biodegradation test (Fig. 6) are similar and show no new bands or either, band displacement relative to neat PLA. This behavior agrees with that observed by Arrieta et al. [21] and Rudnik et al. [27].

The three strong absorption bands characteristic of PLA shown in Fig. 6 are due to the vibrations of the C–CO–O–C group [37]. These three bands are the axial strain band of the C=O (carbonyl bond) at 1748  $\text{cm}^{-1}$ ; the axial strain band of the C–O bond at 1267  $\text{cm}^{-1}$ ; and the asymmetric axial strain C–O–C at 1081 and 1130  $\text{cm}^{-1}$ .

After 90, 120 and 150 days of soil exposure, the carbonyl index of all samples was calculated and presented in Table 3.

It can be observed that there was a difference in the absorbance intensity at  $1749\text{ cm}^{-1}$ , corresponding to the carbonyl group (C=O), in relation to the reference band at  $1451\text{ cm}^{-1}$ , when the films were buried in the garden soil. This change in intensity of the carbonyl bands is caused by the action of extracellular hydrolytic enzymes produced by bacteria and fungi present in the soil microbiota. According to the literature [3, 27, 37], the decrease in intensity of the carbonyl bands with the composting time interval shows that the degradation of PLA occurred at the ester group of the long molecular chains.

Nevertheless, a significant decay in the carbonyl index with composting time interval, attributed to enzymatic hydrolysis during biodegradation test, was observed only for neat PLA and PLA/CNC/TW20. Since neat PLA did not show the highest disintegration rate (Fig. 4), another biodegradation mechanism, associated to enzymatic oxidation of the shorter chains and/or hydroxyl groups to form carbonyl groups in the polymer backbone [35, 37–41], is occurring simultaneously. Therefore, the existence of two concurring chemical mechanisms of biodegradation justify these results and the measurements of carbonyl index of samples did not corroborate with previous analysis.

## Conclusions

Results confirmed that surfactants can enhance biodegradation rate of neat PLA or PLA/CNC nanocomposites. Among PLA/CNC/S films prepared with the TWEEN and SPAN surfactants, the most prominent disintegration rate and decay was observed for PLA/CNC/SP20 film. Taking into account that SPAN 20 is hydrophobic/lipophilic because its HLB value is lower than 10, the hydrophilic nature of surfactants was not a determinant property to enhance PLA/CNC biodegradation rate. Conversely, the surfactant molecular weight behaved as a determinant parameter to enhance the biodegradation rate of PLA/CNC/S composite. Nevertheless, for surfactants belonging to the same chemical family, the highest biodegradation rate for PLA/CNC/S composites obeys the principle of high HLB, and low spherulite size. In this work, the low crystallinity of PLA/CNC/S, and low molecular weight of the surfactant also contributed to enhance biodegradation rate of composites. Therefore, if the addition of surfactants with different chemical groups in polymeric matrices are being evaluated, the molecular weight, degree of crystallinity and spherulite size of polymer matrix need to be taken into account since these properties counterbalance the surfactant HLB value.

**Acknowledgements** The authors gratefully acknowledge Foundation for Science and Technology of the State of Pernambuco (FACEPE) for their financial support of this study. Thanks are also due to the Biomaterials and Biosystems Laboratory (LAMAB/UFPB) and Polymer Materials and Characterization Laboratory (LMPC/UFPB) for sample characterizations.

## References

1. Lima RMR, Romeiro Filho E (2003) The ergonomics analysis contribution for the product project directed towards recycling. *Rev Prod* 13(2):82–87 (in portuguese)

2. Franchetti SMM, Marconato JC (2006) Biodegradable polymers—a partial way for decreasing the amount of plastic waste. *Quím Nova* 29(4):811–816 (in portuguese)
3. Lv S, Liu X, Gu J, Jiang Y, Tan H, Zhang Y (2017) Microstructure analysis of polylactic acid-based composites during degradation in soil. *Int Biodeterior Biodegrad* 122:53–60
4. Suryanegara L, Nakagaito AN, Yano H (2009) The effect of crystallization of PLA on the thermal and mechanical properties of microfibrillated cellulose-reinforced PLA composites. *Comp Sci Technol* 69(7–8):1187–1192
5. Petersson L, Kvien I, Oksman K (2007) Structure and thermal properties of poly(lactic acid)/cellulose whiskers nanocomposite materials. *Comp Sci Technol* 67:2535–2544
6. Garlotta DA (2001) Literature review of poly(lactic acid). *J Polym Environ* 9(2):63–84
7. Lemos AL, Martins RM (2014) Development and characterization of polymeric composites based on poly(lactic acid) and natural fibers. *Polimeros* 24:190–197 (in portuguese)
8. Morelli CL, Marconcini JM, Pereira FV, Bretas RES, Branciforti MC (2012) Extraction and characterization of cellulose nanowhiskers from balsa wood. *Macromol Symp* 319(1):191–195
9. Kamal MR, Khoshkava V (2015) Effect of cellulose nanocrystals (CNC) on rheological and mechanical properties and crystallization behavior of PLA/CNC nanocomposites. *Carbohydr Polym* 123:105–114
10. Fortunati E, Luzi F, Puglia D, Dominici F, Santulli C, Kenny JM, Torre L (2014) Investigation of thermo-mechanical, chemical and degradative properties of PLA limonene films reinforced with cellulose nanocrystals extracted from *Phormium tenax* leaves. *Eur Polym J* 56:77–91
11. Fortunati E, Armentano I, Zhou Q, Iannoni A, Saino E, Visai L, Berglund LA, Kenny JM (2012) Multifunctional bionanocomposite films of poly(lactic acid), cellulose nanocrystals and silver nanoparticles. *Carbohydr Polym* 87:1596–1605
12. Emami Z, Meng Q, Pircheraghi G, Manas-Zloczower I (2015) Use of surfactants in cellulose nanowhisker/epoxy nanocomposites: effect on filler dispersion and system properties. *Cellulose* 22:3161–3176
13. Heux L, Chauve G, Bonini C (2000) Nonflocculating and chiral-Nematic self-ordering of cellulose microcrystals suspensions in nonpolar solvents. *Langmuir* 16(21):8210–8212
14. Fortunati E, Armentano I, Zhou Q, Puglia D, Terenzi A, Berglund LA, Kenny JM (2012) Microstructure and nonisothermal cold crystallization of PLA composites based on silver nanoparticles and nanocrystalline cellulose. *Polym Degrad Stab* 97:2027–2036
15. Dong XM, Revol JF, Gray DG (1998) Effect of microcrystallite preparation conditions on the formation of colloid crystals of cellulose. *Cellulose* 5:19–32
16. Gois GS, Nepomuceno NC, França CHA, Almeida YMB, Hernández EP, Oliveira JE, Oliveira MP, Medeiros ES, Santos ASF (2019) Influence of morphology and dispersion stability of CNC modified with ethylene oxide derivatives on mechanical properties of PLA-based nanocomposites. *Polym Comp* 40:E399–E408. <https://doi.org/10.1002/pc.24704>
17. Lizundia E, Vilas JL, León LM (2015) Crystallization, structural relaxation and thermal degradation in Poly(l-lactide)/cellulose nanocrystal renewable nanocomposites. *Carbohydr Polym* 123:256–265
18. Bondeson D, Oksman K (2007) Dispersion and characteristics of surfactant modified cellulose whiskers nanocomposites. *Comp Interfaces* 14(7–9):617–630
19. Kim J, Montero G, Habibi Y, Hinestroza JP, Genzer J, Argyropoulos DS, Rojas OJ (2009) Dispersion of cellulose crystallites by nonionic surfactants in a hydrophobic polymer matrix. *Polym Eng Sci* 49:2054–2061
20. Silviya EK, Unnikrishnan G, Varghese S, Guthrie JT (2013) Surfactant effects on poly(ethylene-co-vinyl acetate)/cellulose composites. *Comp Part B Eng* 47:137–144
21. Arrieta MP, Fortunati E, Dominici F, Rayón E, López J, Kenny JM (2014) PLA-PHB/cellulose based films: mechanical, barrier and disintegration properties. *Polym Degrad Stab* 107:139–149
22. Li Z, Hu X, Shi J, Zou X, Huang X, Zhou X et al (2016) Bacteria counting method based on polyaniline/bacteria thin film. *Biosens Bioelectron* 81:75–79
23. Szabo JG, Meiners G, Heckman L, Rice EW, Hall J (2017) Decontamination of *Bacillus* spores adhered to iron and cement mortar drinking water infrastructure in a model system using disinfectants. *J Environ Manag* 187:1–7
24. Arrieta MP, López J, López D, Kenny JM, Peponi L (2015) Development of flexible materials based on plasticized electrospun PLA-PHB blends: structural, thermal, mechanical and disintegration properties. *Eur Polym J* 73:433–446

25. Haque MM, Puglia D, Fortunati E, Pracella M (2017) Effect of reactive functionalization on properties and degradability of poly(lactic acid)/poly(vinyl acetate) nanocomposites with cellulose nanocrystals. *React Funct Polym* 110:1–9
26. Souza PMS, Morales AR, Mei LHI, Morales MAM (2014) Estudo da influência de argilas organofílicas no processo de biodegradação do PLA. *Polimeros* 24(1):110–116 (in portuguese)
27. Rudnik E, Briassoulis D (2011) Degradation behaviour of poly(lactic acid) films and fibres in soil under mediterranean field conditions and laboratory simulations testing. *Ind Crops Prod* 33(3):648–658
28. Farah S, Anderson DG, Langer R (2016) Physical and mechanical properties of PLA, and their functions in widespread applications—a comprehensive review. *Adv Drug Deliv Rev* 107:367–392
29. Gois GS, Andrade MF, Garcia SMS, Vinhas GM, Santos ASF, Medeiros ES, Oliveira JE, Almeida YMB (2017) Soil biodegradation of PLA/CNW nanocomposites modified with ethylene oxide derivatives. *Mat Res* 20(Suppl. 2):899–904. <https://doi.org/10.1590/1980-5373-MR-2016-0960>
30. Arrieta MP, López J, Rayón E, Jiménez A (2014) Disintegrability under composting conditions of plasticized PLA-PHB blends. *Polym Degrad Stab* 108:307–318
31. Dolores SM, Patricia AM, Santiago F, Juan L (2014) Influence of biodegradable materials in the recycled polystyrene. *J Appl Polym Sci* 131(23):1–7
32. Fortunati E, Peltzer M, Armentano I, Torre L, Jiménez A, Kenny JM (2012) Effects of modified cellulose nanocrystals on the barrier and migration properties of PLA nano-biocomposites. *Carbohydr Polym* 90:948–956
33. Arrieta MP, Fortunati E, Domínic F, Rayón E, López J, Kenny JM (2014) Multifunctional PLA-PHB/cellulose nanocrystal films: processing, structural and thermal properties. *Carbohydr Polym* 107:16–24
34. Gois GS (2018) Investigation of biodegradable composites based on poly(lactic acid) with cellulose nanocrystals modified with dicumyl peroxide and surfactants. PhD thesis, Federal University of Pernambuco (in portuguese). <https://repositorio.ufpe.br/bitstream/123456789/31935/1/TESE%20Gelsonide%20da%20Silva%20Gois.pdf>
35. Luzi F, Fortunati E, Puglia D, Petrucci R, Kenny JM, Torre L (2015) Study of disintegrability in compost and enzymatic degradation of PLA and PLA nanocomposites reinforced with cellulose nanocrystals extracted from *Posidonia Oceanica*. *Polym Degrad Stab* 121:105–115
36. Gu J-D, Ford T, Thorp K, Mitchell R (1996) Microbial growth on fiber reinforced composite materials. *Int Biodeterior Biodegrad* 37:197203
37. Drumond WS, Wang SH, Mothé CG (2004) Synthesis and characterization of copoly(lactic acid-b-ethylene glycol). *Polím Cienc Tecnol* 14(2):74–79 (in portuguese)
38. Latos-Brozio M, Masek A (2020) The effect of natural additives on the composting properties of aliphatic polyesters. *Polymers* 12(9):1856
39. Zain AHM, Ab Wahab MK, Ismail H (2018) Biodegradation behaviour of thermoplastic starch: the roles of carboxylic acids on cassava starch. *J Polym Environ* 26:691–700
40. Salazar-Sánchez MR, Campo-Eraza SD, Villada-Castillo HS, Solanilla-Duque JF (2019) Structural changes of cassava starch and polylactic acid films submitted to biodegradation process. *Int J Biol Macromol* 129:442–447
41. Kale G, Kijchavengkul T, Auras R, Rubino M, Selke SE, Singh SP (2007) Compostability of bioplastic packaging materials: an overview. *Macromol Biosci* 7(3):255–277

**Publisher's Note** Springer Nature remains neutral with regard to jurisdictional claims in published maps and institutional affiliations.

Springer Nature or its licensor (e.g. a society or other partner) holds exclusive rights to this article under a publishing agreement with the author(s) or other rightsholder(s); author self-archiving of the accepted manuscript version of this article is solely governed by the terms of such publishing agreement and applicable law.